

PROCEEDINGS OF SPIE

[SPIDigitalLibrary.org/conference-proceedings-of-spie](https://spiedigitallibrary.org/conference-proceedings-of-spie)

Target detection in SAR images using codifference and directional filters

Kaan Duman
A. Enis Çetin

Target detection in SAR images using codifference and directional filters

Kaan Duman^a and A. Enis Çetin^a

^a Dept. of Electrical and Electronics Engineering, Bilkent University, 06800, Ankara, Turkey

ABSTRACT

Target detection in SAR images using region covariance (RC) and codifference methods is shown to be accurate despite the high computational cost. The proposed method uses directional filters in order to decrease the search space. As a result the computational cost of the RC based algorithm significantly decreases. Images in MSTAR SAR database are first classified into several categories using directional filters (DFs). Target and clutter image features are extracted using RC and codifference methods in each class. The RC and codifference matrix features are compared using l_1 norm distance metric. Support vector machines which are trained using these matrices are also used in decision making. Simulation results are presented.

Keywords: Synthetic aperture radar (SAR) images, automatic target recognition (ATR) and classification, directional filters (DFs), region covariance (RC) matrix, region codifference matrix, support vector machine (SVM)

1. INTRODUCTION

Unlike infrared or optical sensors, synthetic aperture radar (SAR) sensors are able to produce the images of terrains under any weather conditions at any time of day and night. Automatic detection and recognition of man-made (metal) objects in SAR images has been an active research area in recent years. There are many areas of application in which the detection or recognition of a target or texture signal is important in SAR images. These applications include detection and classification for military purposes, recognition of the terrain surface for mineral exploration, determining the spilled oil boundaries in oceans and extracting the sea state and ice hazard maps for navigators.^{1,2}

A typical and complete automatic target recognition (ATR) system includes detection, discrimination, classification, recognition and identification stages. The method proposed in this paper can be used in the detection or discrimination stages of a SAR ATR system.

In this paper, a pre-processing stage based on directional filtering is introduced for the SAR target detection algorithm proposed earlier³ involving the region covariance (RC) and codifference methods which use various distance measures including normalized l_1 norm distance metrics for making decisions. Directional filters were successfully used as a first stage in many applications including vector quantization, image coding.⁴⁻⁸ Regions of interests (ROIs) in SAR images which are simply determined based on the amplitude information are filtered using two-dimensional directional-wavelet type filters in order to divide both the target and clutter (non-target) images into categories according to their orientations.

The output of the pre-processing stage is fed to a detection stage in which representative feature parameters are extracted using the covariance and codifference matrices of the ROIs. The entire process is illustrated in Fig. 1. Pre-processing and target detection stage boxes will be investigated in the following sections. An advantage of using covariance and codifference matrices is their small dimension compared to the size of ROIs. In addition, the speckle noise in SAR images is reduced by the natural averaging operation during the computation of these matrices. It is observed that the directional approach, when used with l_1 norm distance metric, reduces the computational complexity without decreasing much the target detection accuracy in publicly available MSTAR (moving and stationary target recognition) database. Target detection and false alarm rates are comparable to the method in Ref. 3 which has high computational cost. The RC and codifference matrices are also used as feature space parameters for support vector machines (SVM) for discrimination between target and clutter images in each directional category. SVM classifiers provide least computational solutions in real-time applications for the SAR image classification problem, when the training phase is avoided.

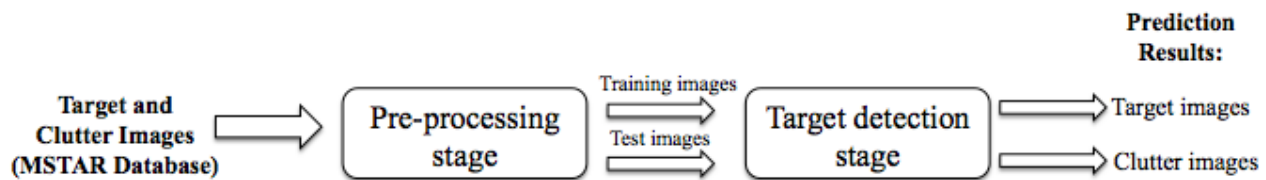


Figure 1. The target detection process investigated in this paper.

The remaining part of the paper is planned as follows. Section 2 introduces the directional filters (DFs) used in this work and the pre-processing stage of the algorithm. In Section 3, target detection using region covariance and codifference with different feature matching methods are described. In Section 4, simulation results are presented and the proposed method is compared to other existing methods.

2. PRE-PROCESSING STAGE AND DIRECTIONAL FILTER (DF) DESIGN

The number of comparisons made in matching with targets and clutters cause a considerable computational cost in Ref. 3. The computational cost is mainly due to the straightforward distance computations with high number of training samples. The computational cost has to be reduced when scanning large regions at different locations. In addition, the target detection algorithm is expected to be used in real-time applications. In this article a pre-processing stage is proposed which consists of applying directional filters to classify target images to categories according to their orientations. Since a smaller number of images is used within categories in decision of target or clutters, the computational cost of target detection algorithm significantly decreases with the proposed pre-processing stage.

MSTAR database includes images of targets and clutters.⁹ Target images consist of the armored personal carriers BMP-2, BTR-70 and T-72 main battle tank. Images of open fields, farms, trees, roads and buildings form the clutter images. The target images are provided in 128-by-128 pixel size chips. The clutter images are cropped in this size from the original 1476-by-1784 sized images. Several target and clutter image samples are shown in Figure 2. Target images are available in all orientations in the database.

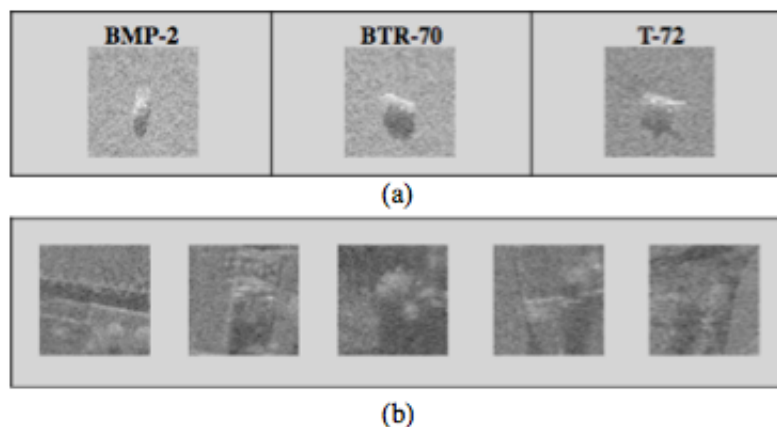


Figure 2. Several target and clutter images: (a) Target images of size 128-by-128, (b) Clutter images of size 128-by-128.

The design principle of the DFs used in this work is illustrated in Fig. 3. On the left hand side, 7-by-7 horizontal DF is shown. This filter is used as the template filter to design the other DFs. Along the horizontal

axis, the filter coefficient values change from -1 to 1 in 7 steps in a linear manner. The other directional filters are produced from the template filter coefficient matrix by rotation. To obtain the first filter DF1 from the template DF, the outermost pixels are rotated clockwise by one unit as shown in Fig. 3. The second filter DF2 is obtained from DF1 in a similar manner. In DF2, the inner filter coefficients are also rotated clockwise by one step. The DF3 is obtained from the DF2, and it is a diagonal filter. The DF4 and the DF5 are 90° rotated versions of DF1 and DF2, respectively. Filters DF6-DF10 are symmetric with respect to DF1-DF5 on vertical axis, respectively. All the DFs are shown in Fig. 3.

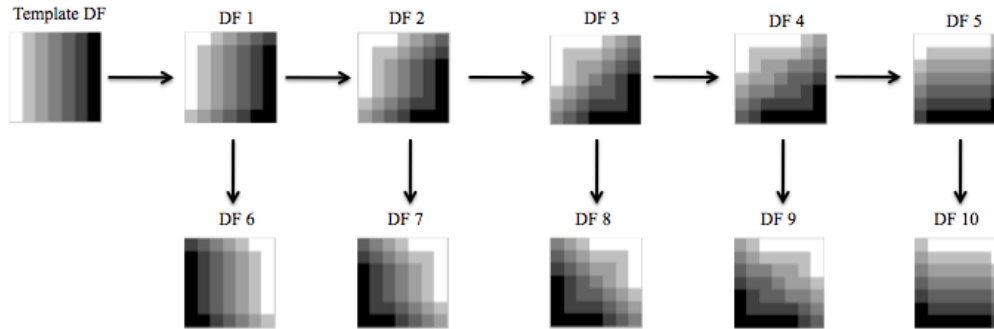


Figure 3. Design of the directional filters (DFs).

As it can be observed from the sample target and clutter images in Fig. 2, the objects in SAR images are brighter to the top of them, providing natural vertical edges for all the ROIs. This property of the SAR images provides the images to be accurately classified into categories, as DF1-DF10 are designed to pick up the images having vertical edges between -90° and 90° rotation in 10 steps. However, a sharp vertical filter is avoided, because it tends to bring up more images to its category than the other filters. Similarly, a sharp horizontal filter (see template DF in Fig. 3) tends to bring less number of images to its category compared to DF1-DF10.

In Fig. 4, the block diagram of the pre-processing stage is presented. First, the original 128-by-128 input target images obtained from the MSTAR database are cropped such that the targets and their shades are covered in the new 64-by-64 images. If the original image is depicted by I , $I(45 : 108, 33 : 96)$ represent the 64-by-64 image cropped. These 64-by-64 images are chosen simply because processing them is less costly and the studies in Ref. 3 show that they give close detection performances to the 128-by-128 images. Then, these cropped images are decimated by a factor of two in each dimension before applying the directional filters in order to match the DF size with the targets. To prevent aliasing a simple 3-by-3 low-pass Gaussian filter is used during decimation. The coefficients of this filter, H_{LPF} is as follows,

$$H_{LPF} = \begin{bmatrix} \frac{1}{16} & \frac{1}{8} & \frac{1}{16} \\ \frac{1}{8} & \frac{1}{4} & \frac{1}{8} \\ \frac{1}{16} & \frac{1}{8} & \frac{1}{16} \end{bmatrix}$$

After applying DFs, the l_1 norm of the output images are calculated as $M_R = ||R(x,y)||_1$, where M_R represents the magnitude of the image region R . Finally, the cropped images are categorized under the number of the filter that they give the highest norm. As a result, the n^{th} category contains the 64-by-64 target images that produces the highest l_1 energy output to DF n . Same operations are also applied to 128-by-128 clutter images obtained from the MSTAR database. The cropped 64-by-64 target and clutter images form the ROIs.

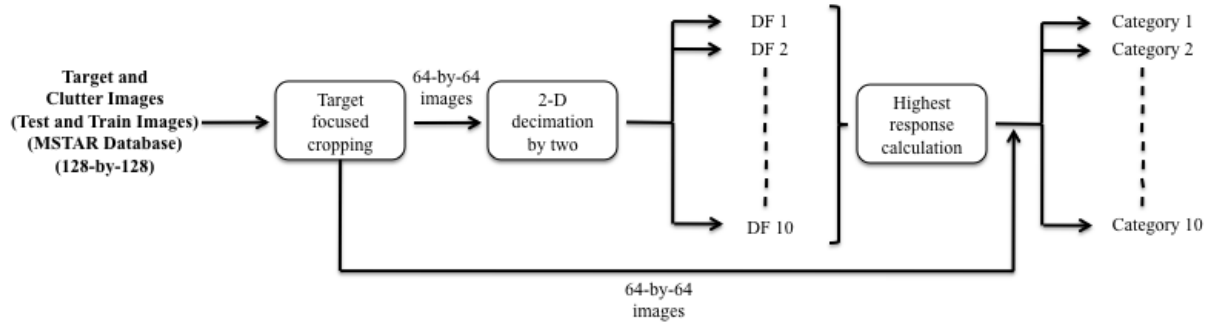


Figure 4. Block diagram of the pre-processing stage.

3. CODIFFERENCE METHOD AND TARGET DETECTION STAGE

After distributing the images into categories, training and test datasets are formed from the images. Then, in each category, for each ROIs of the clutter and target images, RC and codifference matrices are extracted.

3.1 Region Covariance (RC) and Codifference Matrices

The covariance and the codifference matrices of an image are computed by extracting a feature vector for each pixel in the ROI. The feature vector used in this work is defined as follows:

$$z_k = \left[x \quad y \quad I(x, y) \quad \frac{dI(x, y)}{dx} \quad \frac{dI(x, y)}{dy} \quad \frac{d^2 I(x, y)}{dx^2} \quad \frac{d^2 I(x, y)}{dy^2} \right] \quad (1)$$

where, k is the label of a pixel, (x, y) is the position of a pixel, I is intensity of a pixel (as gray scale images are used in this work), $dI(x, y)/dx$ is the horizontal and $dI(x, y)/dy$ is the vertical derivative of the ROI calculated through the filter $[-1 \ 0 \ 1]$, $d^2 I(x, y)/dx^2$ is the horizontal and $d^2 I(x, y)/dy^2$ is the vertical second derivative of the ROI calculated through the filter $[-1 \ 2 \ -1]$. For example, for a 4 by 4 region, $k = 1, 2, \dots, 16$; $x = -2, 1, 0, 1$. One should note that in filtering processes, there is no need for computationally costly multiplications, as the result can be found out by addition and subtraction of the shifted sequences of input data.

Let the feature vector be represented as follows:

$$z_k = [z_k(i)]^T \quad (2)$$

where, $z_k(i)$ is the i^{th} entry of the feature vector z_k . The 7-by-7 covariance matrix CR of a ROI R is defined by the fast covariance matrix computation formula:

$$C_R = [c_R(i, j)] = \left(\frac{1}{n-1} \left[\sum_{k=1}^n (z_k(i)z_k(j)) - \frac{1}{n} \sum_{k=1}^n z_k(i) \sum_{k=1}^n z_k(j) \right] \right) \quad (3)$$

where n is the total number of pixels in the ROI and $c_R(i, j)$ is the $(i, j)^{th}$ component of the covariance matrix. The covariance and codifference matrices are computed using the integral image concept in a computationally efficient manner. This method has the same calculation complexity for all window sizes after computing the integral images.¹⁰

Computational cost of a covariance matrix becomes heavy, when it comes to scanning big regions at different scales and locations. Moreover, many video applications need low computational costs to present real-time solutions. In order to decrease the computational cost, the codifference matrix is introduced.¹¹ The codifference matrix is defined as follows:

$$C_R = [c_R(i, j)] = \left(\frac{1}{n-1} \left[\sum_{k=1}^n (z_k(i) \oplus z_k(j)) - \frac{1}{n} \sum_{k=1}^n z_k(i) \oplus \sum_{k=1}^n z_k(j) \right] \right) \quad (4)$$

In the codifference matrix, the scalar multiplications in the covariance matrix calculation are changed with an additive operator \oplus . The operator \oplus is simply a summation operation with the same sign as the multiplication operation result. For real numbers a and b , the operator \oplus is defined as in the following equation:

$$a \oplus b = \text{sign}(a \times b)(|a| + |b|) \quad (5)$$

Since $a \oplus b = b \oplus a$, the codifference matrix is also symmetric like the RC matrix. The codifference matrix behaves similar to the covariance matrix. For two variables, the sign of the result for the operations in covariance and codifference is the same. If two variables' signs are the same, the output is positive and if they are not, the output is negative. In many computer systems, addition is less costly compared to multiplication. This makes the calculation of the codifference matrix computationally efficient compared to the covariance matrix.

The operator \oplus satisfies totality, associativity and identity properties; therefore it is a monoid function. In other words it is a semigroup with identity property. Similar statistical methods are used in literature.¹² Another similar statistical function is the Average Magnitude Difference Function (AMDF), which is widely used in speech processing to determine periodicity of voiced sounds.

3.2 Target Detection Strategy

Using the extracted RC and codifference matrices' values as features, two methods are considered in the decision of whether an image belongs to a target or clutter. The RC and codifference matrices are symmetric, and therefore the upper (or lower) triangle of the matrices carry sufficient information for making decisions.

The first method involves distance computation through l_1 norm. The l_1 norms of the differences between the two covariance or codifference matrices' feature vectors are used in decision of whether a test image is a target or clutter image. The l_1 norm distance metric ρ is defined in the following equation.

$$\rho(C_1, C_2) = \sum_{i=1}^p \left[\sum_{j=1}^p (|C_1(i, j) - C_2(i, j)|) \right] \quad (6)$$

where, C_1, C_2 is the covariance or codifference matrix of ROIs R_1 and R_2 belong to a test and training image in a category and p is the number of items in the feature vector z in Eq. 1. For a test image, the l_1 norm distances are calculated with every training image in its category. If the smallest distance is obtained from a target training image, then the test image is detected as a target image. If not (i.e. smallest distance is acquired from a clutter training image), then the image is predicted as a clutter image. This metric calculates only the magnitude of the difference of matrices obtained from the images. It is chosen because it provides the simplest decision metric with high target detection performance like the other metrics used in Ref. 3.

For making comparisons with the l_1 norm distance metric method, matrix coefficients are also used as feature parameters in support vector machines (SVM).¹³ In each category a different SVM is designed. In all simulations, polynomial kernel is used in SVMs. The matrix coefficients of test images are compared to the model generated in training phase. The final predictions are obtained according to the classification results of the SVMs which determine whether the input test image is a target image or a clutter image.

The block diagram of the target detection stage in each category is shown in Figure 5.

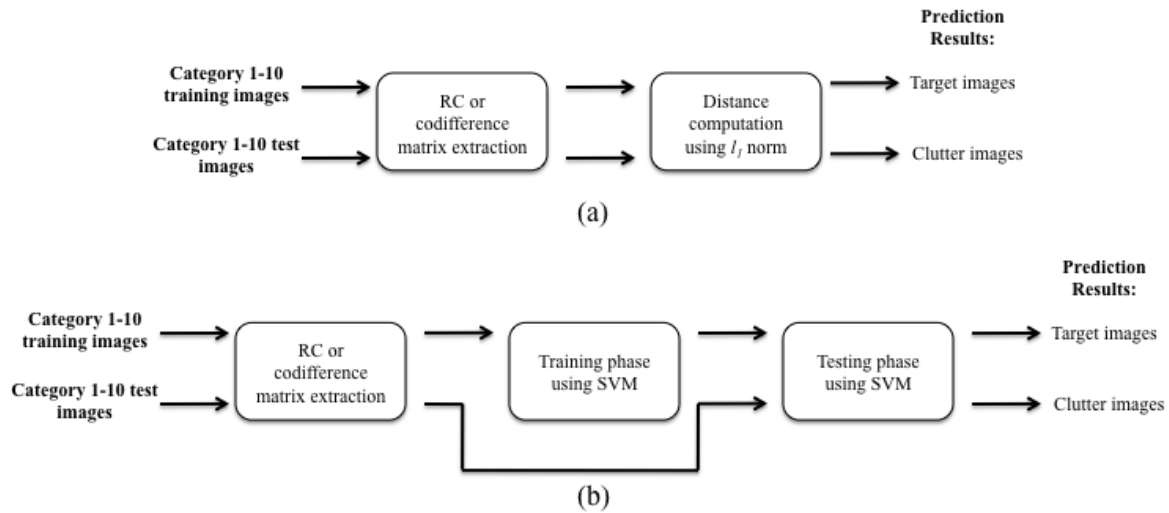


Figure 5. Block diagram of the target detection stage applied in each category using (a) l_1 norm distance metric in Eq. 6 (b) SVM classifiers

4. SIMULATION RESULTS

Target and clutter images in the MSTAR database are divided into training and test images. The number of images used for training and testing are shown in Table 1. The proportion of test images to the training images is about 20:1. This high ratio increases the importance of getting an accurate target detection rate.

Table 1. Number of images used in training and testing studies

	Number of training images	Number of test images
Target	132	2627
Clutter	668	13346

As it was explained in Sections 2 and 3, the method presented in this paper has two stages. In this section, the effect of each stage on the overall target detection performance is described in detail.

As indicated before in Fig. 1, the first stage of the algorithm is pre-processing, where target and clutter images belonging to each category are determined using directional filter (DF) outputs. Sample target images belonging to each category are shown in Fig. 6. Symbols of DFs are given above the filters. These symbols are used to simplify the tables presented in this section, as they show the orientation of the DFs. As Fig. 6 illustrates, the symbols show also the orientation of the targets, which are decided according to the DFs' output that they represent.

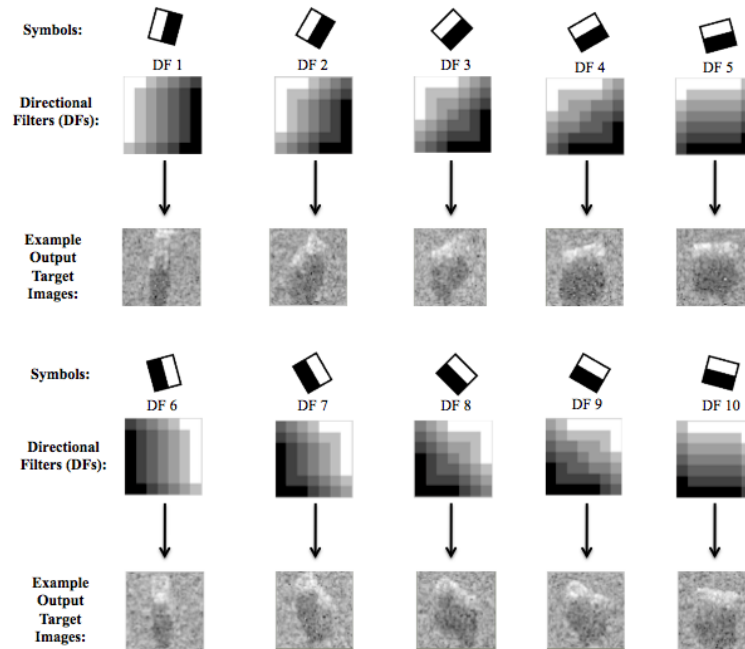






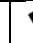
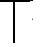
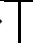
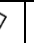


Figure 6. Example target images selected by the directional filters (DFs).

The training images distributed in 10 different categories vary in number, as they are chosen according to the filter responses. During the training stage the target and clutter images shown in Table 1 are classified into categories. However, number of clutter images is reduced to match the number of target images. Therefore, the number of target and clutter images in the training dataset decreased to 10-15 from 132. Eventually, the number of comparisons made between test and training images with l_1 norm distance metric in Eq. 6 is reduced by approximately 90%. This is the main reason for computational efficiency in using the two-stage approach. When the training dataset is put into SVM and models are created for each category, this computational efficiency is no longer available as the total number of images to be trained remains the same.

Exact number of target and clutter training images at the output of DFs 1-10 are given in Table 2. Same number of target and clutter images are used in each category.

Table 2. Number of target and clutter training images in each category after the pre-processing stage with 10 directional filters.

	Categories										
											
	1	2	3	4	5	6	7	8	9	10	Total
Number of training images											
Target	12	15	14	11	14	12	15	11	13	15	132
Clutter	12	15	14	11	14	12	15	11	13	15	132

Target detection stage is the decision making stage of whether a test image is a clutter or target using l_1 norm distance based method and SVMs designed. Simulation results are summarized in Table 3 which includes the target detection and false alarm (incorrectly classified clutter images) rates for each category. The number of target and clutter test images are also given in the denominator part of the results. The simulation results using RC and the codifference matrices are listed in the following table.

Table 3. Target detection and false alarm rates obtained using the RC and the codifference matrix with l_1 norm distance metric and SVM classifiers on 10 categories.






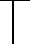
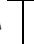
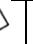


	Categories										
											
	1	2	3	4	5	6	7	8	9	10	Total
Target detection accuracies and false alarm rates											
Using RC method											
With l_1 norm distance metric											
Target det. accuracies	$\frac{137}{140}$	$\frac{338}{338}$	$\frac{302}{304}$	$\frac{213}{213}$	$\frac{305}{321}$	$\frac{142}{142}$	$\frac{358}{358}$	$\frac{275}{275}$	$\frac{194}{194}$	$\frac{336}{342}$	$\frac{2600}{2627}$ (98.97%)
False alarm rates	$\frac{5}{1401}$	$\frac{0}{654}$	$\frac{3}{842}$	$\frac{14}{877}$	$\frac{23}{2924}$	$\frac{9}{1359}$	$\frac{1}{610}$	$\frac{0}{755}$	$\frac{0}{955}$	$\frac{12}{2969}$	$\frac{67}{13346}$ (0.50%)
With SVM classifiers											
Target det. accuracies	$\frac{137}{140}$	$\frac{338}{338}$	$\frac{297}{304}$	$\frac{213}{213}$	$\frac{291}{321}$	$\frac{142}{142}$	$\frac{358}{358}$	$\frac{275}{275}$	$\frac{192}{194}$	$\frac{338}{342}$	$\frac{2581}{2627}$ (98.25%)
False alarm rates	$\frac{4}{1401}$	$\frac{0}{654}$	$\frac{6}{842}$	$\frac{35}{877}$	$\frac{93}{2924}$	$\frac{15}{1359}$	$\frac{0}{610}$	$\frac{0}{755}$	$\frac{6}{955}$	$\frac{2}{2969}$	$\frac{161}{13346}$ (1.21%)
Using region codifference method											
With l_1 norm distance metric											
Target det. accuracies	$\frac{138}{140}$	$\frac{338}{338}$	$\frac{304}{304}$	$\frac{213}{213}$	$\frac{311}{321}$	$\frac{142}{142}$	$\frac{358}{358}$	$\frac{275}{275}$	$\frac{194}{194}$	$\frac{342}{342}$	$\frac{2615}{2627}$ (99.54%)
False alarm rates	$\frac{0}{1401}$	$\frac{1}{654}$	$\frac{0}{842}$	$\frac{1}{877}$	$\frac{0}{2924}$	$\frac{6}{1359}$	$\frac{3}{610}$	$\frac{0}{755}$	$\frac{0}{955}$	$\frac{5}{2969}$	$\frac{16}{13346}$ (0.12%)
With SVM classifiers											
Target det. accuracies	$\frac{137}{140}$	$\frac{338}{338}$	$\frac{299}{304}$	$\frac{212}{213}$	$\frac{310}{321}$	$\frac{142}{142}$	$\frac{358}{358}$	$\frac{275}{275}$	$\frac{193}{194}$	$\frac{340}{342}$	$\frac{2604}{2627}$ (99.12%)
False alarm rates	$\frac{0}{1401}$	$\frac{1}{654}$	$\frac{2}{842}$	$\frac{3}{877}$	$\frac{2}{2924}$	$\frac{8}{1359}$	$\frac{9}{610}$	$\frac{3}{755}$	$\frac{0}{955}$	$\frac{36}{2969}$	$\frac{64}{13346}$ (0.48%)

Table 3 shows that codifference method delivers high detection accuracies and low false alarm rates compared to the RC method. Furthermore, it has a lower computational complexity compared to the RC method. The general detection performance also rises when l_1 norm distance metric is used instead of SVM classifiers.

As it can be seen in Table 3, there are more target and clutter images in categories 5 and 10 which correspond to $+\Pi/12$ and $-\Pi/12$ degree angles with respect to the vertical axis, respectively. Although the region codifference did not suffer much from this, the RC method has a poor performance in categories 5 and 10. In the second set of simulations, filters 5 and 10 are excluded and only eight filters are used, in order to improve SAR image classification performance. Number of training images in each category obtained using eight directional filters is given in Table 4. The simulation results on eight categories are summarized in Table 5.

Table 4. Number of target and clutter training images in each category after the pre-processing stage with 8 directional filters.








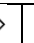
	Categories								
									
	1	2	3	4	6	7	8	9	Total
Number of training images									
Target	12	15	14	28	12	15	11	25	132
Clutter	12	15	14	28	12	15	11	25	132

Table 5. Target detection and false alarm rates obtained using the RC and the codifference matrix with l_1 norm distance metric and SVM classifiers on 8 categories.

	Categories								
	1	2	3	4	6	7	8	9	Total
Target detection accuracies and false alarm rates									
Using RC method									
With l_1 norm distance metric									
Target det. accuracies	$\frac{137}{140}$	$\frac{338}{338}$	$\frac{303}{305}$	$\frac{533}{541}$	$\frac{142}{142}$	$\frac{358}{358}$	$\frac{276}{276}$	$\frac{519}{527}$	$\frac{2606}{2627}$ (99.20%)
False alarm rates	$\frac{5}{1408}$	$\frac{0}{661}$	$\frac{3}{862}$	$\frac{1}{3750}$	$\frac{9}{1366}$	$\frac{1}{621}$	$\frac{0}{771}$	$\frac{7}{3907}$	$\frac{26}{13346}$ (0.19%)
With SVM classifiers									
Target det. accuracies	$\frac{137}{140}$	$\frac{338}{338}$	$\frac{298}{305}$	$\frac{531}{541}$	$\frac{142}{142}$	$\frac{358}{358}$	$\frac{276}{276}$	$\frac{519}{527}$	$\frac{2599}{2627}$ (98.93%)
False alarm rates	$\frac{4}{1408}$	$\frac{0}{661}$	$\frac{6}{862}$	$\frac{0}{3750}$	$\frac{15}{1366}$	$\frac{0}{621}$	$\frac{0}{771}$	$\frac{2}{3907}$	$\frac{27}{13346}$ (0.20%)
Using region codifference method									
With l_1 norm distance metric									
Target det. accuracies	$\frac{138}{140}$	$\frac{338}{338}$	$\frac{305}{305}$	$\frac{540}{541}$	$\frac{142}{142}$	$\frac{358}{358}$	$\frac{276}{276}$	$\frac{527}{527}$	$\frac{2624}{2627}$ (99.89%)
False alarm rates	$\frac{0}{1408}$	$\frac{1}{661}$	$\frac{0}{862}$	$\frac{0}{3750}$	$\frac{6}{1366}$	$\frac{3}{621}$	$\frac{0}{771}$	$\frac{1}{3907}$	$\frac{11}{13346}$ (0.08%)
With SVM classifiers									
Target det. accuracies	$\frac{137}{140}$	$\frac{338}{338}$	$\frac{300}{305}$	$\frac{535}{541}$	$\frac{142}{142}$	$\frac{358}{358}$	$\frac{276}{276}$	$\frac{525}{527}$	$\frac{2611}{2627}$ (99.39%)
False alarm rates	$\frac{0}{1408}$	$\frac{1}{661}$	$\frac{2}{862}$	$\frac{3}{3750}$	$\frac{8}{1366}$	$\frac{9}{621}$	$\frac{3}{771}$	$\frac{49}{3907}$	$\frac{78}{13346}$ (0.58%)

As depicted in Table 4, by eliminating the neighboring categories, number of training images in categories 4 and 9 are increased from 11 and 13 to 28 and 25. This provides higher number of feature vectors for deciding whether the test images in these categories are targets or clutters. Therefore, target detection rates increase and the false alarm rates decrease for the RC and codifference methods. The rise in detection performance is more clear for the RC method. However, the target detection performance of the region codifference method is still better than the RC method. Likewise, the results obtained using l_1 norm distance metric are superior to the results obtained with SVM classifiers.

It is also possible to increase the target detection performance by eliminating DFs and hence further decreasing the number of categories. Naturally, the best rates are achieved when single category is used for target and clutter images as in Ref. 3. It is observed that when the images are distributed to 8 or 10 categories, total target detection performances degrade, but they are still comparable to the results in Ref. 3. Besides, the computational cost of the algorithm Ref. 3 is much higher because a given test image has to be compared to all the images in the training set with normalized l_1 norm distance metrics. In this case, features of the test dataset are compared to a lower number of features in the training dataset using l_1 norm distance metric.

5. CONCLUSIONS

The use of directional filters with the region covariance (RC) and codifference method to detect metal (man-made) objects in SAR images is described in this paper. SAR images used in this work are supplied from the publicly available Moving and Stationary Target Recognition (MSTAR) database. The images in the database include targets (armored personal carriers and a tank) and clutters. l_1 norm distance metric and SVMs are used in decision making. Directional filtering makes it possible to classify target and clutters into different categories according to their geometrical orientations.

The codifference matrix parameters provide better description of SAR images compared to the region covariance matrix originally introduced by Porikli et. al.¹⁴ The calculation of codifference matrix is also less costly compared to RC matrix.

The computational cost of the proposed method is much lower than our earlier method in Ref. 3, when l_1 norm distance metric is used. This is due to the use of directional filters which reduces the number of training

images to be compared in decision making process. Besides, in decision making, l_1 norm distance metric method produces better SAR image classification results than SVM classifiers.

ACKNOWLEDGMENTS

This work is supported by European Commission Seventh Framework Program with EU Grant: 244088 (FIRE-SENSE) and by TÜBİTAK with MİLDAR Project (No. 107A011).

REFERENCES

- [1] Curlander, J. C. and McDonough, R. N., [*Synthetic Aperture Radar - Systems and Signal Processing*], John Wiley & Sons, Inc., New York (1991).
- [2] Oliver, C. and Quegan, S., [*Understanding Synthetic Aperture Radar Images*], Scitech Publishing, Inc., Raleigh, NC (2004).
- [3] Duman, K., Eryıldırım, A., and Çetin, A. E., "Target detection and classification in sar images using region covariance and co-difference," in [*Algorithms for Synthetic Aperture Radar Imagery XVI*], *Proc. SPIE* **7337** (May 2009).
- [4] Ramamurthi, B. and Gersho, A., "Classified vector quantization of images," *IEEE Transactions on Communications* **34**, 1105–1115 (Nov. 1986).
- [5] Gerek, O. N. and Çetin, A. E., "A 2-D orientation-adaptive prediction filter in lifting structures for image coding," *IEEE Transactions on Image Processing* **15**, 106–111 (Jan. 2006).
- [6] Do, M. N. and Vetterli, M., "The contourlet transform: an efficient directional multiresolution image representation," *IEEE Transactions on Image Processing* **14**(12), 2091–2106 (2005).
- [7] Peyre, G. and Mallat, S., "Discrete bandelets with geometric orthogonal filters," in [*Image Processing (ICIP '05)*], *Proc. IEEE* **1**, 1–65–8 (Sept. 2005).
- [8] Viola, P. and Jones, M., "Robust real-time face detection," *International Journal of Computer Vision* **57**, 137–154 (2004).
- [9] Center for Imaging Science (CIS), "MSTAR (Moving and Stationary Target Recognition) SAR database," <http://cis.jhu.edu/data.sets/MSTAR/>.
- [10] Porikli, F. and Tuzel, O., "Fast construction of covariance matrices for arbitrary size image windows," in [*Image Processing (ICIP '06)*], *Proc. IEEE*, 1581–1584 (Oct. 2006).
- [11] Tuna, H., Onaran, I., and Çetin, A. E., "Image description using a multiplier-less operator," *IEEE Signal Processing Letters* **16**, 751–753.
- [12] Akgül, T., Sun, M., Schlaß, R. J., and Çetin, A. E., "Characterization of sleep spindles using higher order statistics and spectra," *IEEE Transactions on Biomedical Engineering* **47**, 997–1009 (Aug. 2000).
- [13] Chang, C.-C. and Lin, C.-J., "LIBSVM: a library for support vector machines," <http://www.csie.ntu.edu.tw/~cjlin/libsvm/> (2001).
- [14] Tuzel, O., Porikli, F., and Meer, P., "Region covariance: A fast descriptor for detection and classification," in [*Computer Vision (ECCV '06)*], *Proc. ECCV*, 367–379 (May 2006).